Electronic Supplementary Material (ESI) for Journal of Materials Chemistry B.

Supporting Information

PD-1 Engineered Cytomembrane Cloaked Molybdenum Nitride for Synergistic Photothermal and Enhanced Immunotherapy of Breast Cancer

Lian Zhu[a], Jia-Lin Liu[a], Jiang-Tao Yang[b], Ding-Wei Wu[b], Na Xu[b], Kai-Fu Huo[c*], Hai-Bo Wang[a*]*

Appendix:

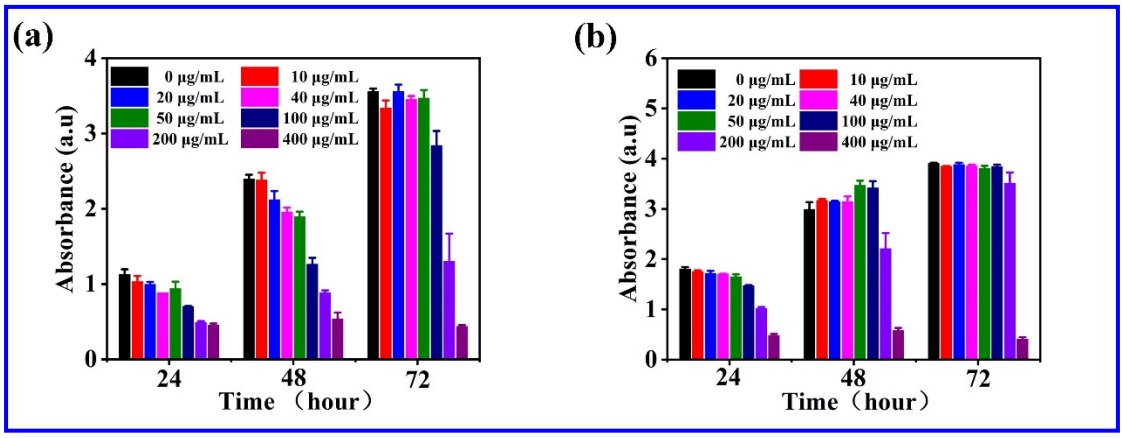

Fig. S1. CCK-8 assay determination of the biocompatibility of synthesized MoN nanomaterials. (a, b) respectively referred to NIH 3T3 and HUVEC cells.

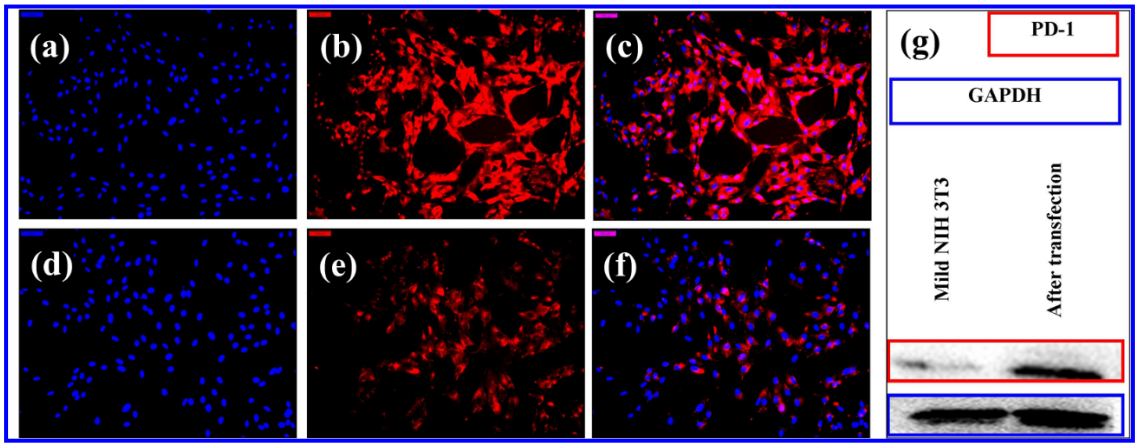

Fig. S2. Characterization of PD-1 protein expression level. (a-c) Fluorescence images of the transfected NIH 3T3 cells. (d-f) Fluorescence images of the mild NIH 3T3 cells. (g) PD-1 protein characterization via western blot. Scale bars in Fig S2a-f refer to 50 μm.

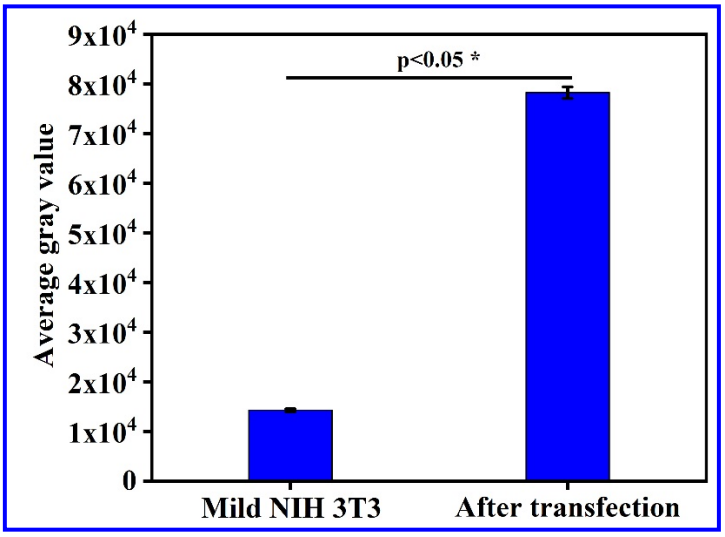

Fig. S3. Quantitative statistics of western blot results, average gray value of PD-1 expression level of NIH 3T3 cells before and after transfection.

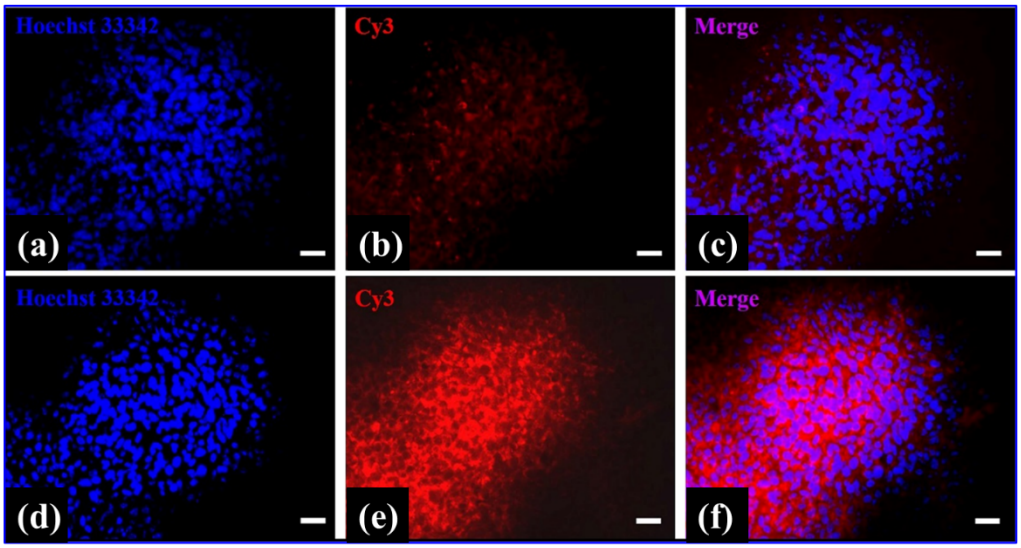

Fig. S4. Fluorescence images of PD-L1 protein expression in vivo research. (a-c) Fluoresence images of PD-L1 in the blank group. (d-f) Fluoresence images of PD-L1 in the MoN@Me&PD-1 group.

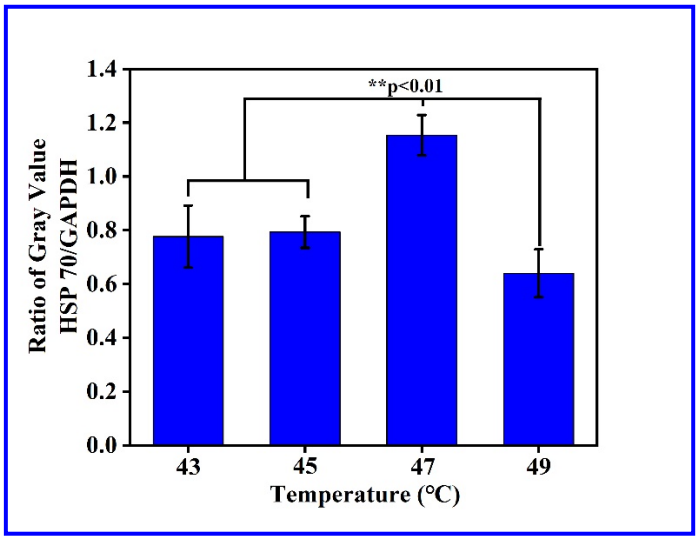

Fig. S5. Quantitative statistics of HSP 70 expression level under different temperature

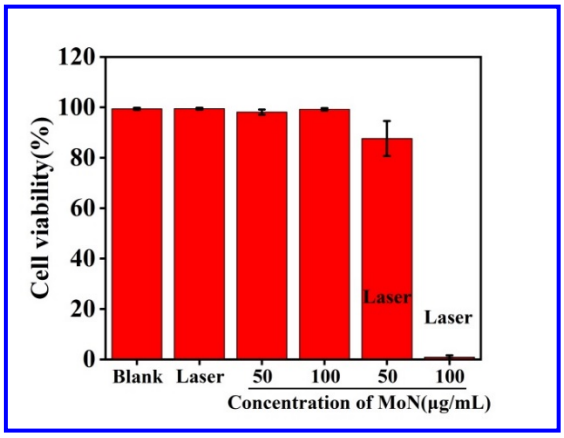

Fig. S6. Quantitative statistics of 4T1 cell viability after phototherapy..

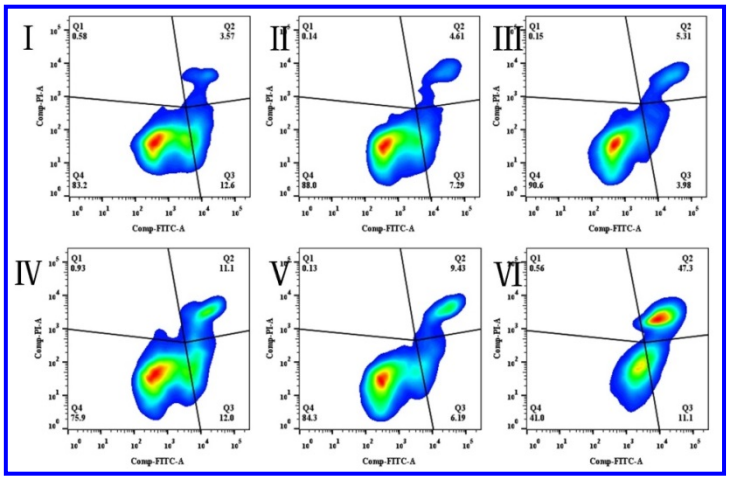

Fig. S7. Flow cytometry characterization of the apoptosis of 4T1 cell after phototherapy.

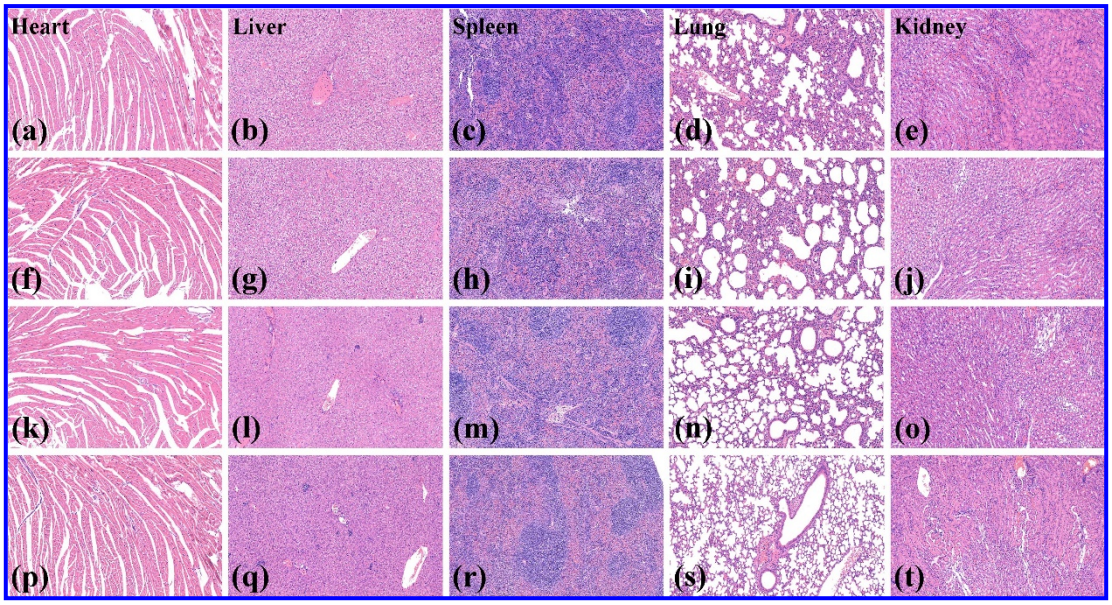

Fig. S8. Characterization the biocompatibility of different therapeutic agents. (a-e) HE staining of heart, liver, spleen, lung and kidney of the blank group. (f-j) HE staining of heart, liver, spleen, lung and kidney of the laser group. (k-o) HE staining of heart, liver, spleen, lung and kidney of the MoN@Me group. (p-t) HE staining of heart, liver, spleen, lung and kidney of the MoN@Me&PD-1 group.

Table S1. Determination of biochemistry indexes of mouse among different groups.

Group	CR (mmol/L)	ALT(U/L)	AST(U/L)	UA(μmol/L)	CK(U/L)	UREA (mmol/L)	Tbil (μmol/L)
Blank	8.04±0.45	110.29±0.83	313.60±0.12	91.04±1.70	1221.59±8.72	15.64±0.028	4.84±0.27
Laser	13.45±0.21	159.92±2.48	446.60±2.70	123.95±1.36	1025.12±0.97	22.70±0.67	11.78±0.23
MoN@Me	10.24±0.02	42.52±1.28	206.87±1.24	62.77±7.24	801.68±2.10	14.02±0.46	4.15±0.057
MoN@Me&PD-1	17.426±0.03	96.58±2.36	169.50±1.18	53.33±1.36	1134.59±8.42	11.55±0.77	5.78±0.076

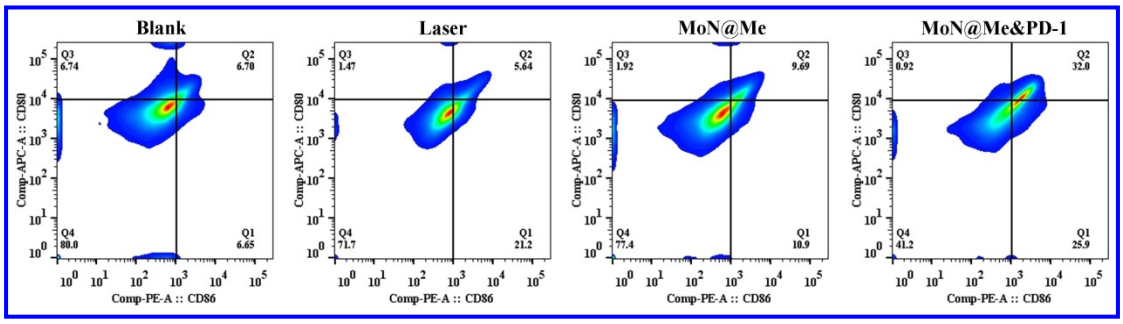

Fig. S9. Detection of DCs maturation via flow cytometry.

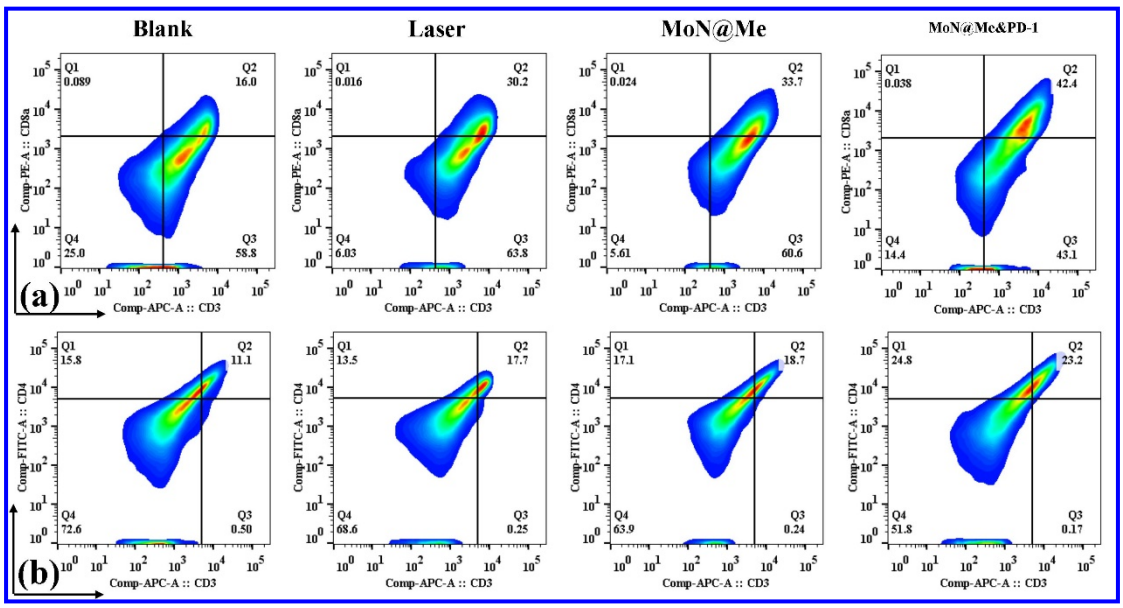

Fig. S10. a, b) T cells activation ratio among different groups.

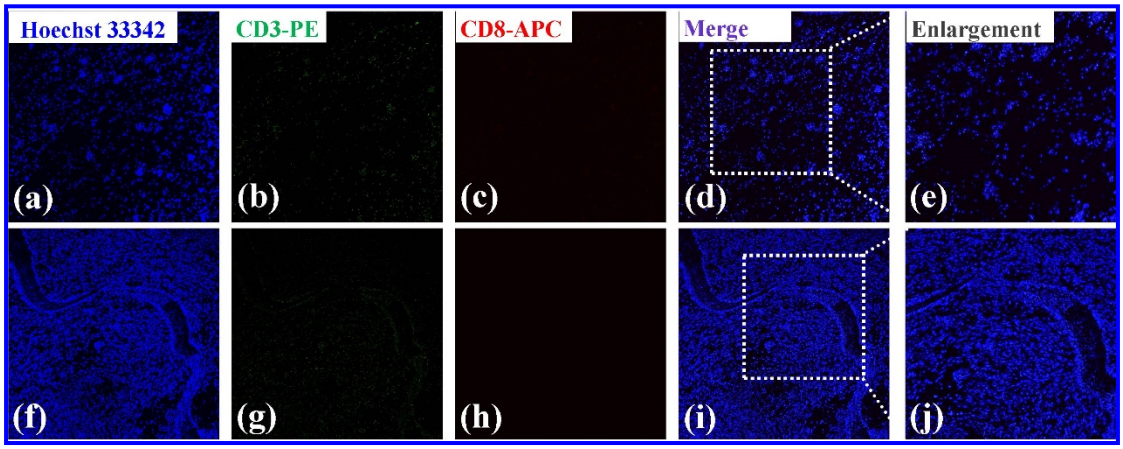

Fig. S11. Fluorescence images confirmation of the CD8+ T cells infiltrating into the tumor tissues among the laser and MoN@Me group.